Rutherford Laboratory
CHILTON, DIDCOT, OXON. OX11 0QX

RL-78-070

Spallation Target-Moderator-Reflector Studies on Nimrod

B C Boland A Carne G C Stirling A D Taylor

November 1978

RL-78-070

SPALLATION TARGET-MODERATOR-REFLECTOR STUDIES ON NIMROD

B C Boland, A Carne, G C Stirling and A D Taylor

ABSTRACT

A mock-up spallation target assembly experiment (MUSTA), designed to assess the optimal conditions for thermal neutron production from proton spallation systems, has been carried out on the Nimrod accelerator under conditions appropriate to the design for the Spallation Neutron Source. The results for neutron production confirm earlier predictions, and are in good agreement with Monte Carlo simulation calculations.

November 1978

CONTENTS

1 INTRODUCTION

A neutron scattering facility, the Spallation Neutron Source (SNS), is being built at the Rutherford Laboratory, designed for research into the atomic and molecular properties of matter using pulsed thermal neutron scattering techniques [1]. The facility is based on a high intensity, high repetition rate proton synchrotron, fast neutrons being produced in short time pulses by the interaction of medium energy protons (∿ 800 MeV) in a heavy metal target. Neutrons are slowed down from source energies (∿ MeV) to energies of interest for neutron scattering (< 10 eV) by thin hydrogenous moderators placed close to the target. Moderator materials, geometries and temperature can be optimised according to neutron spectrum and pulse length requirements. Reflecting material surrounding the target and moderators can reduce neutron leakage and significantly increase yields. To assist in the target-moderator-reflector assembly optimisation, a suite of computer simulation programmes has been established, based on the Monte Carlo transport code TIMOC [2]. To provide experimental benchmark data for these computations, a spallation source has been improvised using the Nimrod accelerator at the Rutherford Laboratory. The aims were to check experimentally the fast neutron production in the target and the coupling of these fast neutrons to the moderator-reflector configuration. The purpose of this report is to summarise the experimental results and comparisons with calculations.

2 EXPERIMENT AND CALCULATIONS

2.1 Neutron Measurements

Protons were extracted into the X3 beam line from Nimrod at a series of energies around the nominal SNS value (720, 800 and 900 MeV). A short (∿ 10 μs) pulse out of a 120 μs spill was directed onto the target by a kicker magnetic system. A Secondary Emission Chamber detector, calibrated by aluminium foil activation, was used to monitor the number of protons incident on the target. Typical intensities of ∿ 0.8 10^{10} protons per pulse in a 10 μs pulse and ∿ 0.4 10^{10} protons per pulse in a 6 μs pulse were achieved.

The primary target consisted of a series of depleted uranium plates clad in Zircaloy-2, mounted in two stainless steel vessels. The first vessel, constituting the front half of the target, contained uranium plates of nominal dimensions 8 cm x 8 cm x 0.6 cm thick, spaced by 0.2 cm cooling channels. The second vessel, the rear half of the target, contained plates 8 cm x 8 cm x 1.2 cm thick with 0.2 cm cooling channels. (figure 1). The system was designed to allow the front half of the target to be used on its own. Cooling was by N_2 gas, D_2O or H_2O. A non-fissile target, a solid 8 cm x 8 cm x 30 cm lead block mounted in a similar steel vessel, was also available. Both vessels had thin windows over the area of the proton beam.

Thin hydrogenous moderators (∿ 10 cm x 10 cm x 5 cm) were used to slow down the fast neutrons produced in the target to thermal energies. Moderator materials were H_2O, polyethylene (CH_2), and H_2O 'poisoned' with a 1 mm Cd sheet situated 1 cm inside the 10 cm x 10 cm face. The moderator was either viewed in 'slab' or 'wing' geometry - in slab geometry the target is viewed directly through the moderator, in wing the moderator is located above the target (figures 1 and 2). In wing geometry, it was possible to surround the moderator with a neutron reflecting material in order to increase the target-moderator coupling efficiency [3,4]. Two sizes of graphite reflector ('Large Graphite Reflector', figure 3, and 'Small Graphite Reflector', figure 4) and a beryllium/graphite reflector ('MUSTA-Beryllium Reflector', figure 5) were used. The moderator was located in a flared exit port of neutron absorbing material, (figure 1). This decoupler neutronically isolates the moderator from its surroundings below a certain energy and reduces pulse broadening from the long time return of slow neutrons from the reflector. Decoupling materials used were natural B_4C (11 mm thickness, ρ = 2.4 g cm^{-3}) and 1.5 mm Cd mounted on an aluminium former. The nominal cut-off energies were 170 eV and 0.5 eV respectively.

The moderator was viewed at a distance of 5.56 m (wing geometry) by a U^{235} fission chamber, and at a distance of 7.25 m (wing geometry) by a vertical 2.5 cm diameter 70 cm Hg, BF_3 detector (figure 6). Borated resin collimators in the 2 m shielding wall served to define the neutron beam. Great care was

taken to ensure that all surfaces viewed by the detector in the target cell, other than the moderator itself, were B_4C shielding. The active area of the fission chamber, defined by the last borated collimator, was 16 cm^2, that of the BF_3 was limited to 0.95 cm^2 by a B_4C shield. Provision was made for locating a 7 cm diameter Ge crystal in the beam, set such that the 220 planes diffracted into a time focussed array of 4 atmosphere He^3 detectors at an angle of 150^o. The BF_3 detector and the crystal analyser could not be used together. The spectrometer area was shielded with Cd faced borated resin blocks on all sides save one, an open back to the cave being the most effective beam dump.

Time-of-flight analysis was performed on the direct beam (fission chamber and BF_3 detector) or on the direct and diffracted beams when the Ge crystal was present (fission chamber and He^3 bank). In addition to these time-analysed detectors, total yield probes for fast neutrons (sulphur pellets and polyethylene disks) and for epithermal neutrons (gold foils) were deployed in the neighbourhood of the target/moderator.

2.2 Thermal and Epithermal Neutron Yields

The time spectrum measured by the BF_3 and fission chamber detectors allows the energy spectrum of the moderated neutrons to be determined for a given target-moderator-reflector configuration. Typical raw data, normalised to 10^{12} protons incident on the target, are shown in figure 7. Background counts, defined as the signal with the moderator removed, are also presented.

Let $M(t)^{MOD}$ be the normalised count at time t in a time channel of width τ_{ch} with the moderators present and $M(t)^{BKD}$ be the background count. Then $\Phi(E)$, the vector flux at energy E per source neutron of neutrons around the normal to the 10 x 10 cm^2 face of the moderator may be computed as follows. First M'(t), the time signal in the absence of air attentuation is calculated using the appropriate scattering and absorption cross-sections.

$$M'(t) = (M(t)^{MOD} - M(t)^{BKD}) \exp\left(4.38 \times 10^{-4} R + \frac{2.13\ 10^{-5} R}{\sqrt{E}}\right)$$

where R is the flight path in cm.

This may then be related to $\phi(E)$:

$$E\Phi(E) = \frac{0.723\ R^3\ M'(t)\ 10^{-12}}{2AY\ \eta(E)\ \tau_{ch}\ E^{\frac{1}{2}}}$$

where A is the area of the detector in cm^2

η is the detector efficiency

Y is the yield of neutrons per proton in the target (taken to be 23.5, 27 and 32 at proton energies of 720 MeV, 800 MeV and 900 MeV respectively for the 30 cm uranium target [3])

and E is the energy associated with time t thus

$t = 0.723\ R\ E^{-\frac{1}{2}}\ \mu s\ cm^{-1}\ eV^{\frac{1}{2}}$

This expression may be simplified for the BF_3 detector,

$$\eta^{BF_3} = 1 - e^{-0.03/\sqrt{E}} \simeq 0.03/\sqrt{E}$$

to

$$E\Phi(E) = \frac{0.723\ R^3\ M'(t)\ 10^{-12}}{0.06\ A\ Y\ \tau_{ch}}$$

Thus the data of figure 7 may be presented as a vector flux per source neutron, $\Phi(E)$ (figure 8).

The data of figure 8 may be characterised by fitting two functions. In the range 300 meV < E < 1 eV (the epithermal region) the functional form,

$$\Phi(E) = C\ E^{-(1-\alpha)}$$

with C and α as parameters, is used. In the thermal region, the data are fitted to a Maxwellian

$$\Phi(E) = \Phi_{th}\ \frac{E}{T^2}\ \exp\{-E/T\}$$

with Φ_{th} and T as parameters. The lethargy exponent, α, is typically ~ 0.16, and T, the effective moderator temperature, ~ 35 meV. Φ_{th} may be interpreted as the integrated thermal yield per source neutron, and C is $E\Phi(E)|_{1eV}$, the flux per unit lethargy per source neutron at 1 eV.

2.3 Monte Carlo Simulation

A number of the experimental configurations were simulated by TIMOC [5]. Neutrons were transported from an initial fast neutron spectrum through the slowing down region using ENDF/B-III cross sections. A fast neutron distribution consistent with that calculated by Fullwood et al [6] on the surface of the target was obtained by using a line source at the centre of the target with a fission spectrum distribution having a characteristic temperature of 1.43 MeV. This relatively hard spectrum is softened by transport through the uranium. The TIMOC values of the flux per unit lethargy in the range 1 eV < E < 10^4 eV were used to estimate $E\Phi(E)|^{TIMOC}_{1eV}$. This figure may then be compared with the $E\Phi(E)|^{EXPT}_{1eV}$ determined above.

3 RESULTS

3.1 Test Moderator-Reflector Configurations

The four parameters α, T, Φ_{th} and $E\Phi(E)|^{EXPT}_{1eV}$ (§2.2) summarises the performance of a given target-reflector-moderator assembly. These data are presented in tables I-VI for the various configurations. Data from the fission chamber, although of poorer statistical quality, were in general agreement. The value for $E\Phi(E)|^{TIMOC}_{1eV}$ as calculated by TIMOC is given for comparison in the final column of each table.

The error associated with the absolute value of $E\Phi(E)|^{EXPT}_{1eV}$ is 20%, due mostly to proton normalisation uncertainties. That associated with $E\Phi(E)|^{TIMOC}_{1eV}$ is 10%, although unknown systematics may still exist in the Monte Carlo results due to uncertainties in the spatial and spectral distribution of primary neutrons.

3.1.1 Large Graphite Reflector Assembly (Table I)

Table I gives data for the set of target coolants used with the Large Graphite Reflector, and a comparison is made with the values obtained without reflector.

In addition, a TIMOC value for the coupling of fast neutrons to a 'bare' moderator (ie a moderator + line source with no other material present) is given to indicate the enhancement due to the target itself and its associated cooling wings (figure 9). A simulation of an enlarged graphite reflector, with additional graphite below the target and the decoupling energy reduced to 50 eV, is given to put the other results in context (figure 10). It is seen that the figure quoted for the SNS conceptual design [1] of 2.5 10^{-4} n ster^{-1} n_f^{-1} for $E\Phi(E)|_{1eV}$ is almost achieved, even with the superior performance of D_2O or Be as a reflector still in hand.

3.1.2 Reflector Changes (Table II)

Of the four configurations studied, the Large Graphite Reflector was, as predicted by TIMOC calculations, the most effective. The Small Graphite Reflector and the MUSTA-Beryllium Reflector (a combination of a limited number of beryllium blocks supplemented by graphite) proved to be comparable. It should be stressed that, although no explicit reflector material was present in the 'No Reflector' case, the target itself and its extensive cooling wings contribute substantially to the reflection into the moderator of fast neutrons leaking from the system.

3.1.3 Moderator Changes (Table III)

The higher proton density of polyethylene (CH_2) makes this moderator more efficient both at 1 eV and in the thermal region. The ratio

$$\Phi_{th}/E\Phi(E)|_{1eV}$$

is 6.0 and 4.6 for CH_2 and H_2O respectively. The effective temperature of a reflected moderator was consistently higher than the unreflected case,

CH_2 being higher than H_2O. All effective temperatures are higher than the physical temperature (25 meV).

While the intensity of the Cd poisoned moderator was reduced only slightly in the slowing down region, a factor ∿ 8 reduction in thermal neutron output was observed. The corresponding improvement in the time pulse is discussed in §3.3.

3.1.4 Target Changes (Table IV)

In Table IV data are presented normalised to source protons rather than source neutrons, since the neutron to proton ratio is not a constant in this set of experiments. The final column gives the efficiency for neutron production at 720 MeV for each target, as measured by the 1 eV flux, relative to the primary uranium target.

3.1.5 Proton Energy Changes (Table V)

Data are presented normalised to source neutrons using an energy dependent neutron to proton yield of 23.5, 27.0 and 32.0 at 720 MeV, 800 MeV and 900 MeV respectively. The final column of table V gives the relative production of 1 eV neutrons in the moderator for these values of proton energy.

3.1.6 Miscellaneous (Table VI)

A comparison of 'wing' and 'slab' geometries is made in table VI. It should be noted that, due to engineering constraints, a far from optimised 'slab' geometry was used. (The moderator viewed a N_2 gas cooled target at a distance of 10 cm through the cooling wing. In a practical 'slab' geometry, the moderator would be adjacent to the target).

A considerable gain in neutron thermalisation is obtained by reducing the decoupler energy to 0.5 eV (cadmium decoupler). The expected corresponding degradation of the pulse characteristics was, however, not studied.

3.2 Axial Distribution of Fast Neutrons

The fast neutron distribution along the length of the target was monitored by measuring the induced P^{32} activity in an array of sulphur pellets located on the top surface of the target. The reaction $S^{32}(n,p)P^{32}$ has a threshold of 3 MeV and an effective cut off at 15 MeV. By assuming the spectral distribution of fast neutrons given by Fullwood et al [6], an estimate of the spatial distribution of the total fast neutron yield may be obtained. These data are presented in figure 11 for the N_2 cooled uranium target, the D_2O cooled uranium target and the solid lead target. Since the sulphur pellets have finite dimensions (22 mm diameter, 2.5 mm radius) these data represent the convolution of the spatial distribution of fast neutrons with the geometric shape of the probe. The major limitations of these data are that an extrapolation has been made from the high energy component of the spectrum (3 to 15 MeV) which accounts for less than 10% of the total production, and spectral changes due to the presence of coolant have not been taken into account.

3.3 Time Characteristics of the Neutron Pulse

Monochromatic neutrons were selected by diffraction from a single crystal of germanium and their time characteristics studied by time-of-flight. Corresponding to the (220), (440), (660), (880) and (10 10 0) planes of germanium, neutrons of wavelength 3.99 Å, 1.94 Å, 1.29 Å, 0.973 Å and 0.777 Å were obtained (see figure 12). The structure associated with each diffraction peak is indicative of the time structure of the moderator pulse.

In figure 13 the intense, but broad pulse from the 9.8 x 9.8 x 4.8 cm^3 unpoisoned moderator is compared with the sharper pulse obtained by poisoning the moderator at a depth of 1 cm with a 1 mm cadmium sheet. The cadmium decouples the two sections of the moderator so that the Maxwellian build-up in the thick region cannot contribute a long time tail to the pulse. It is found that above ∿ 300 meV, the signals from the two moderators become identical. After removing sources of pulse broadening associated with the spectrometer,

- mosaic spread of the germanium crystal

- flight path uncertainties
- timing uncertainties etc

the intrinsic moderator pulse width as a function of λ may be obtained. These data, together with the intensity penalty for poisoning, are presented in Table VII. The FWHM of the poisoned moderator is comparable with data obtained on the Harwell linac [7] for a 4 cm x 30 cm x 30 cm CH_2 moderator poisoned by gadolinium at a depth of 1.3 cm.

3.4 Radiation Levels

Radiation levels in the spectrometer cave were less than 0.05 mr/hr in 'wing' geometry, but in 'slab' an increase to greater than 3 mr/hr was observed.

The distribution of radioactivity in the neighbourhood of the target was monitored using CH_2 disks and Al foil [8]. Spallation products produced at the front and in the centre of the target were also determined, using an array of thin uranium foils.

4 SUMMARY

Experiments to determine the performance of spallation-based target-moderator-reflector assemblies have been carried out for a variety of configurations under different conditions. Proton energies, target and target coolants, moderators and reflectors have been systematically varied to give estimates of primary neutron production rates, target-moderator coupling coefficients, epithermal and thermal neutron yields, and time characteristics of the slow neutron pulses. The results can be broadly summarised as follows:

- primary neutron production efficiencies (neutrons produced per proton incident on the target) are in agreement with previously reported measurements.
- target-moderator coupling coefficients (parameterised by $E\Phi(E)|_{1eV}$), reflector efficiencies, and moderated-neutron yields are in agreement with values calculated by the Monte-Carlo transport code TIMOC.

- moderated-neutron yields are consistent with figures derived from earlier experimental data for the performance of the Spallation Neutron Source conceptual design.

The results provide confirmation of the predicted SNS performance, and show that TIMOC gives a good description of spallation-based target-moderator systems, so providing an important tool for optimisation of the SNS neutron production assembly.

ACKNOWLEDGEMENTS

The successful outcome of this experiment depended on the combined efforts of a wide group of people. Ron Wimblett took responsibility for engineering design and operation of the target assembly, and was ably assisted by Peter Gregory, Mike Holding, Ken Moye and John Rimen. The kicker magnet was designed and constructed by Robin Elliott. Radiation measurements and monitoring were carried out by David Perry. Ian Gardner planned the special requirements for operating Nimrod, and substantial contributions were made throughout the experiments by the accelerator operations team. Francis Atchison, Mike Johnson and David Mildner contributed much to the scientific planning for the experiment, and Mike Johnson was responsible for implementing the Monte Carlo programs used in assessing the experimental data.

TABLE I

Configuration: H_2O, D_2O and N_2 coolant, with and without Large Graphite Reflector

H_2O Moderator, 9.8 x 9.8 c 4.8 cm^3, B_4C Decoupler

30 cm U Target, E_p = 720 MeV

Wing Geometry

	α	T (meV)	Φ_{th} n_{th} $ster^{-1}$ n_f^{-1}	$E\Phi(E)\|^{EXPT}$ $n\ ster^{-1}$ leV^{-1} n_f^{-1}	$E\Phi(E)\|^{TIMOC}$ $n\ ster^{-1}$ leV^{-1} n_f^{-1}
Large Graphite Reflector					
D_2O Cooled	0.16	37	$5.1\ 10^{-4}$	$1.11\ 10^{-4}$	$1.36\ 10^{-4}$
N_2 Cooled	0.17	38	$4.9\ 10^{-4}$	$1.06\ 10^{-4}$	$1.15\ 10^{-4}$
H_2O Cooled	0.16	37	$4.5\ 10^{-4}$	$0.97\ 10^{-4}$	$0.97\ 10^{-4}$
No Reflector					
D_2O Cooled	0.18	35	$2.8\ 10^{-4}$	$0.62\ 10^{-4}$	$0.74\ 10^{-4}$
N_2 Cooled	0.19	35	$2.2\ 10^{-4}$	$0.49\ 10^{-4}$	$0.53\ 10^{-4}$
H_2O Cooled	0.18	35	$2.3\ 10^{-4}$	$0.52\ 10^{-4}$	$0.52\ 10^{-4}$
Error	±0.01	±1			
Special Simulations					
Line Source + Bare Moderator					$0.22\ 10^{-4}$
Enlarged Graphite Reflector, 50 eV Decoupler, Bottom Reflector					$2.3\ 10^{-4}$

TABLE II

Configuration: Variation of reflector

D_2O Coolant, H_2O Moderator, 9.8 x 9.8 x 4.8 cm^3

B_4C Decoupler, 30 cm U Target

E_p = 720 MeV

Wing Geometry

	α	T (meV)	Φ_{th} n_{th} $ster^{-1}$ n_f^{-1}	$E\Phi(E)\|^{EXPT}$ $n\ ster^{-1}$ leV^{-1} n_f^{-1}	$E\Phi(E)\|^{TIMOC}$ $n\ ster^{-1}$ leV^{-1} n_f^{-1}
Large Graphite	0.16	37	$5.1\ 10^{-4}$	$1.11\ 10^{-4}$	$1.36\ 10^{-4}$
Small Graphite	0.15	37	$4.2\ 10^{-4}$	$0.94\ 10^{-4}$	$1.30\ 10^{-4}$
MUSTA-Beryllium	0.15	38	$4.7\ 10^{-4}$	$0.96\ 10^{-4}$	$1.21\ 10^{-4}$
No Reflector	0.18	35	$2.8\ 10^{-4}$	$0.62\ 10^{-4}$	$0.74\ 10^{-4}$

TABLE III

Configuration: Variation of moderator

B_4C Decoupler, 30 cm U Target,

E_p = 720 MeV

Wing Geometry

	α	T (meV)	Φ_{th} n_{th} ster^{-1} n_f^{-1}	$E\Phi(E)\|^{EXPT}_{1eV}$ n ster^{-1} n_f^{-1}	$E\Phi(E)\|^{TIMOC}_{1eV}$ n ster^{-1} n_f^{-1}
Large Graphite Reflector D_2O Coolant:					
CH_2 10x10x5 cm^3	0.07	40	$7.4\ 10^{-4}$	$1.21\ 10^{-4}$	
H_2O 9.8x9.8x4.8 cm^3	0.16	37	$5.1\ 10^{-4}$	$1.11\ 10^{-4}$	$1.36\ 10^{-4}$
H_2O Cd Poisoned		30	$0.73\ 10^{-4}$	$0.88\ 10^{-4}$	
Large Graphite Reflector N_2 Coolant:					
CH_2 10x10x5 cm^3	0.09	40	$7.0\ 10^{-4}$	$1.15\ 10^{-4}$	
H_2O 9.8x9.8x4.8 cm^3	0.17	38	$4.9\ 10^{-4}$	$1.06\ 10^{-4}$	$1.15\ 10^{-4}$
No Reflector N_2 Coolant:					
CH_2 10x10x5 cm^3	0.10	36	$3.4\ 10^{-4}$	$0.59\ 10^{-4}$	
H_2O 9.8x9.8x4.8 cm^3	0.19	35	$2.2\ 10^{-4}$	$0.49\ 10^{-4}$	$0.53\ 10^{-4}$

TABLE IV

Configuration: Variation of target, with and without reflector

D_2O Coolant, H_2O Moderator, 9.8 x 9.8 x 4.8 cm^3

B_4C Decoupler, 30 cm U Target

E_p = 720 MeV

Wing Geometry

	α	T (meV)	Φ_{th} n_{th} ster^{-1} p^{-1}	$E\Phi(E)\|^{EXPT}_{1eV}$ n ster^{-1} p^{-1}	Relative 1eV neutron flux per proton
Large Graphite Reflector					
Full U Target	0.16	37	$1.2\ 10^{-2}$	$2.6\ 10^{-3}$	1.00
½ U Target	0.15	37	$1.1\ 10^{-2}$	$2.4\ 10^{-3}$	0.92
Pb Target	0.17	36	$0.82\ 10^{-2}$	$1.8\ 10^{-3}$	0.69
No Reflector					
Full U Target	0.18	35	$0.66\ 10^{-2}$	$1.5\ 10^{-3}$	1.00
½ U Target	0.17		$0.59\ 10^{-2}$	$1.3\ 10^{-3}$	0.89

TABLE V

Configuration: Proton energy changes

H_2O Moderator, 9.8 x 9.8 x 4.8 cm^3

30 cm U Target, B_4C Decoupler

Slab Geometry, N_2 Coolant

	α	T (meV)	Φ_{th} n_{th} $ster^{-1}$ n_f^{-1}	$E\Phi(E)\|^{EXPT}_{1eV}$ $n\ ster^{-1}$ n_f^{-1}	Relative 1eV neutron flux per proton
E_p = 720 MeV	0.20	33	$0.94\ 10^{-4}$	$0.22\ 10^{-4}$	1
E_p = 800 MeV	0.23	34		$0.26\ 10^{-4}$	1.38
E_p = 900 MeV	0.18	32		$0.22\ 10^{-4}$	1.40
Error	±.04	±2		±25%	

TABLE VI

Configuration: Miscellaneous

H_2O Moderator, 9.8 x 9.8 x 4.8 cm^3

30 cm U Target, E_p = 720 MeV

	α	T (meV)	Φ_{th} n_{th} $ster^{-1}$ n_f^{-1}	$E\Phi(E)\|^{EXPT}_{1eV}$ $n\ ster^{-1}$ n_f^{-1}	$E\Phi(E)\|^{TIMOC}_{1eV}$ $n\ ster^{-1}$ n_f^{-1}
Large Graphite Reflector D_2O Coolant:					
B_4C Decoupler	0.16	37	$5.1\ 10^{-4}$	$1.11\ 10^{-4}$	$1.36\ 10^{-4}$
Cd Decoupler		44	$10.5\ 10^{-4}$	$1.55\ 10^{-4}$	
No Reflector, N_2 Coolant Position of Moderator:					
Front of Target (wing)	0.19	35	$2.2\ 10^{-4}$	$0.49\ 10^{-4}$	$0.53\ 10^{-4}$
Rear of Target (wing)	0.19	33	$1.6\ 10^{-4}$	$0.37\ 10^{-4}$	
Front of Target (slab)	0.20	33	$0.94\ 10^{-4}$	$0.22\ 10^{-4}$	

TABLE VII

Comparison of Poisoned and Unpoisoned H_2O Moderators

Germanium Reflection	Intensity Penalty (Unpoisoned/ Poisoned)	FWHM Unpoisoned (μs)	FWHM Poisoned (μs)	Resolution FWHM (μs)	Δt Unpoisoned (μs)	Δt Poisoned (μs)
(440) (1.94 Å)	7.6	60	39	31	51	24
(600) (1.29 Å)	9.2	44	28	23	38	16
(800) (0.973 Å)	6.6	40	22	20	35	9
(10 10 0) (0.777 Å)	4.9	28	21	18	21	11

REFERENCES

1 L C W Hobbis, G H Rees and G C Stirling (Eds.), 'A Pulsed Neutron Facility for Condensed Matter Research', Rutherford Laboratory Report RL-77-064 (1977).

2 H Kschwendt and H Rief, 'TIMOC - A General Purpose Monte-Carlo Code for Stationary and Time Dependent Neutron Transport', Euratom Report EUR 4519e (1970).

3 See for example, J M Carpenter, 'Pulsed Spalation Neutron Sources for Slow Neutron Scattering', Nucl. Instrum. Meth. 145, 91 (1977).

4 B C Boland, G C Stirling and A D Taylor, 'Reflector Studies for Pulsed Neutron Moderators', Rutherford Laboratory Report RL-77-140 (1977).

5 M W Johnson and A D Taylor, unpublished work.

6 R R Fullwood, J D Cramer, R A Haarman, R P Forrest and R G Schrandt, 'Neutron Production by Medium-Energy Protons on Heavy Metal Targets', Los Alamos Scientific Laboratory Report LA-4789 (1972).

7 I C Cole and C G Windsor, 'Lineshapes in Pulsed Neutron Powder Diffraction', unpublished work.

8 D R Perry and I Stephenson, to be published.

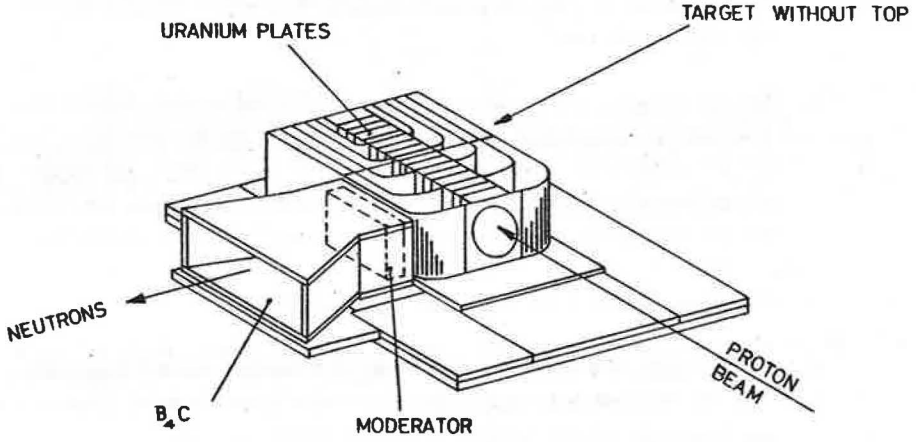

Figure 1. The uranium target showing target plates and cooling channels in the wings. The front end of the target is viewed by a moderator in 'slab' geometry.

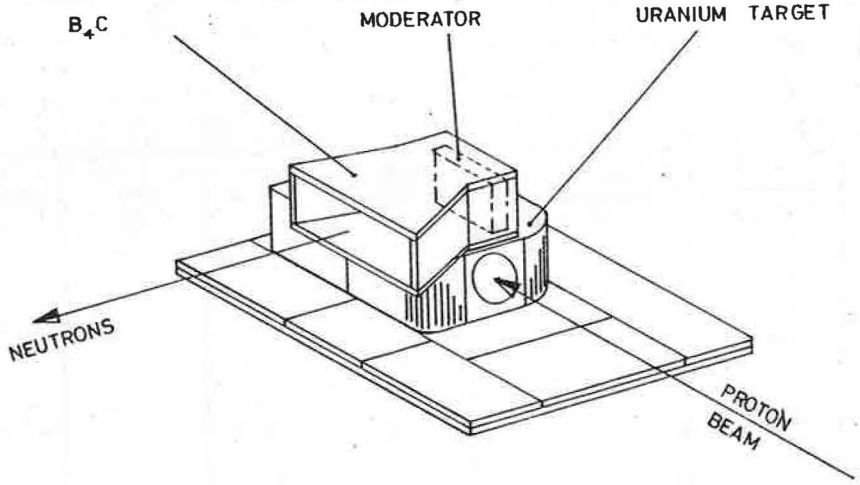

Figure 2. The uranium target. The front end of the target is viewed by a moderator in 'wing' geometry.

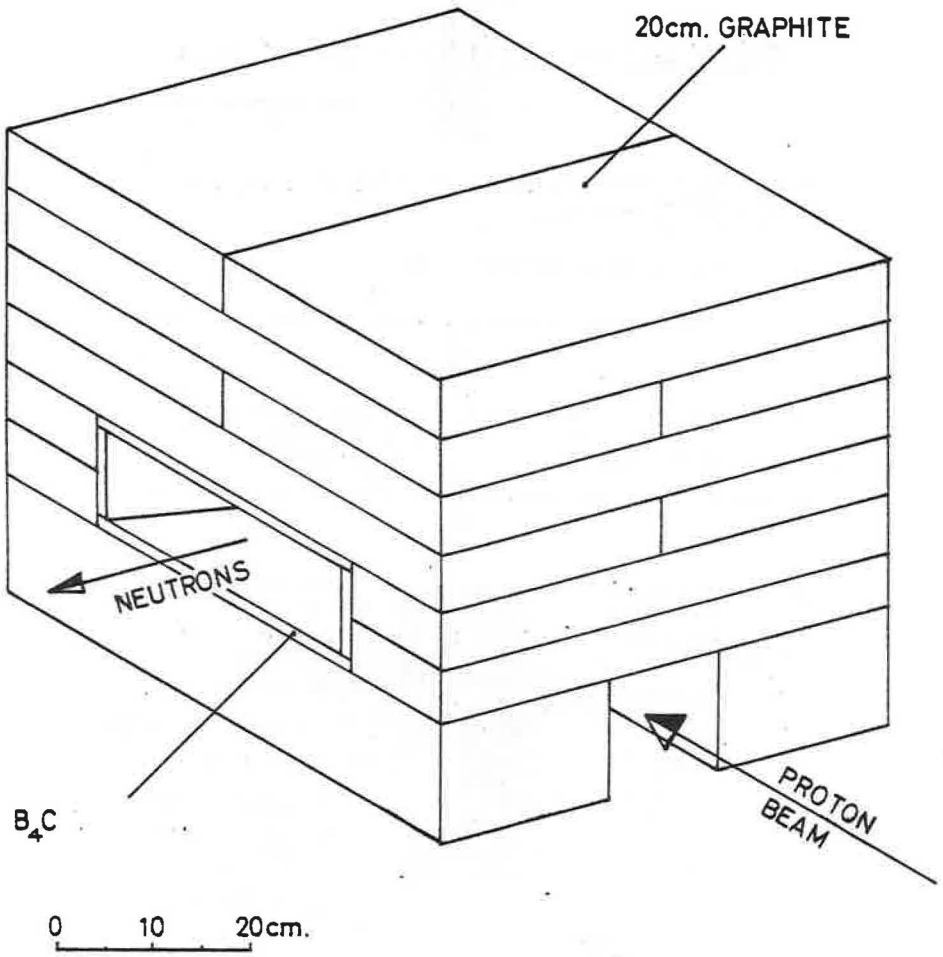

Figure 3. The Large Graphite Reflector configuration. A moderator, decoupled by B_4C, views the target in wing geometry and is surrounded by (approximately) 20 cm of graphite on five sides.

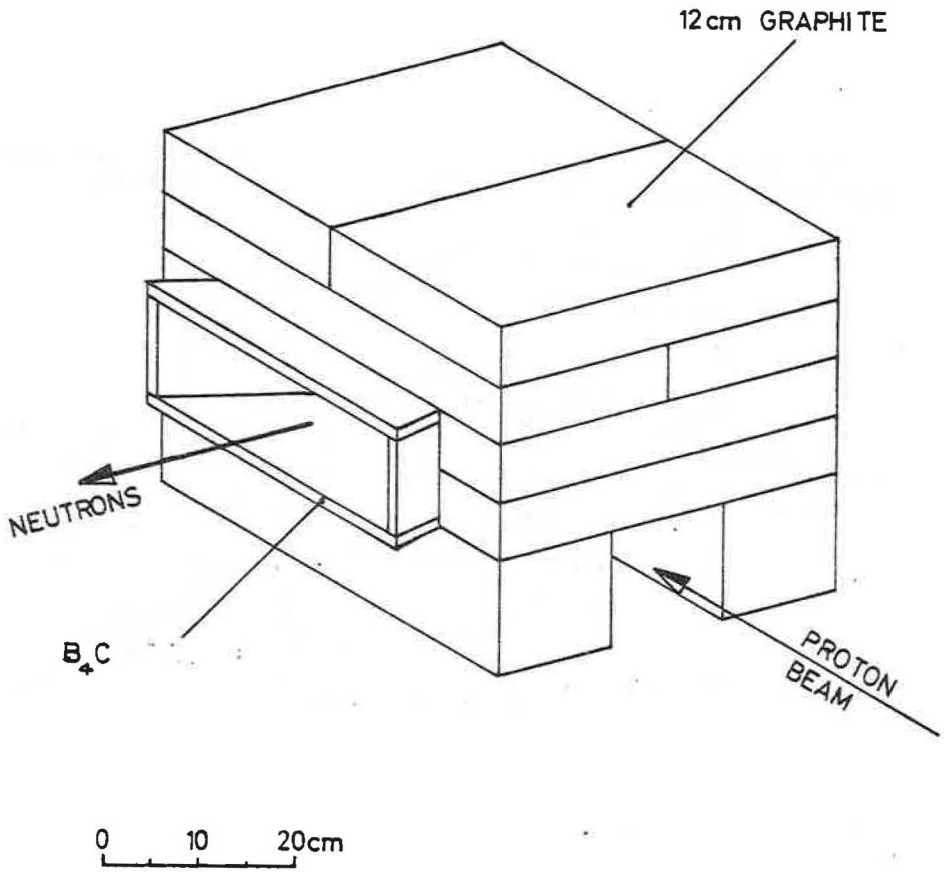

Figure 4. The Small Graphite Reflector configuration. A moderator, decoupled by B_4C, views the target in wing geometry and is surrounded by (approximately) 12 cm of graphite on five sides.

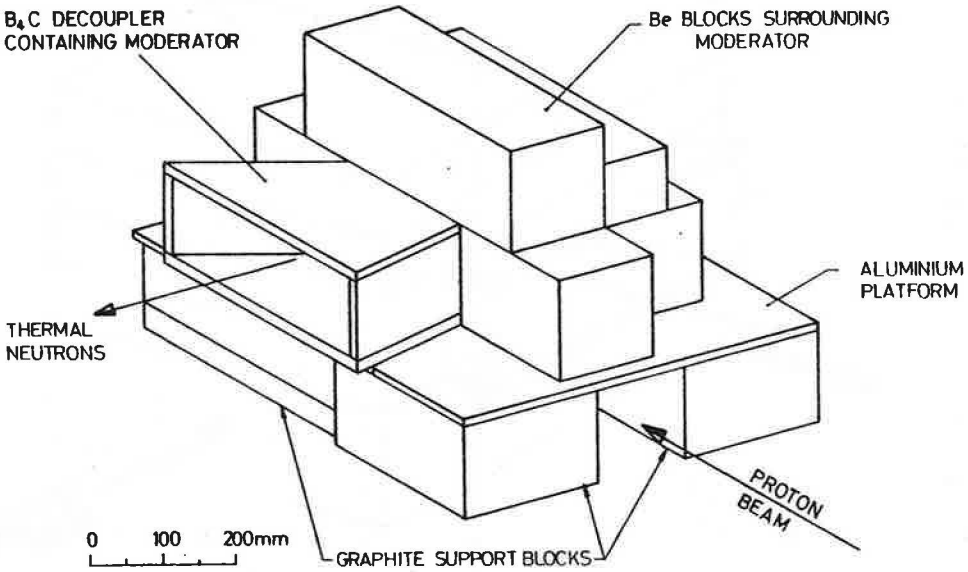

Figure 5. The MUSTA-Beryllium Reflector configuration. A moderator, decoupled by B_4C, views the target in wing geometry. The moderator is surrounded as well as possible with the limited amount of beryllium available.

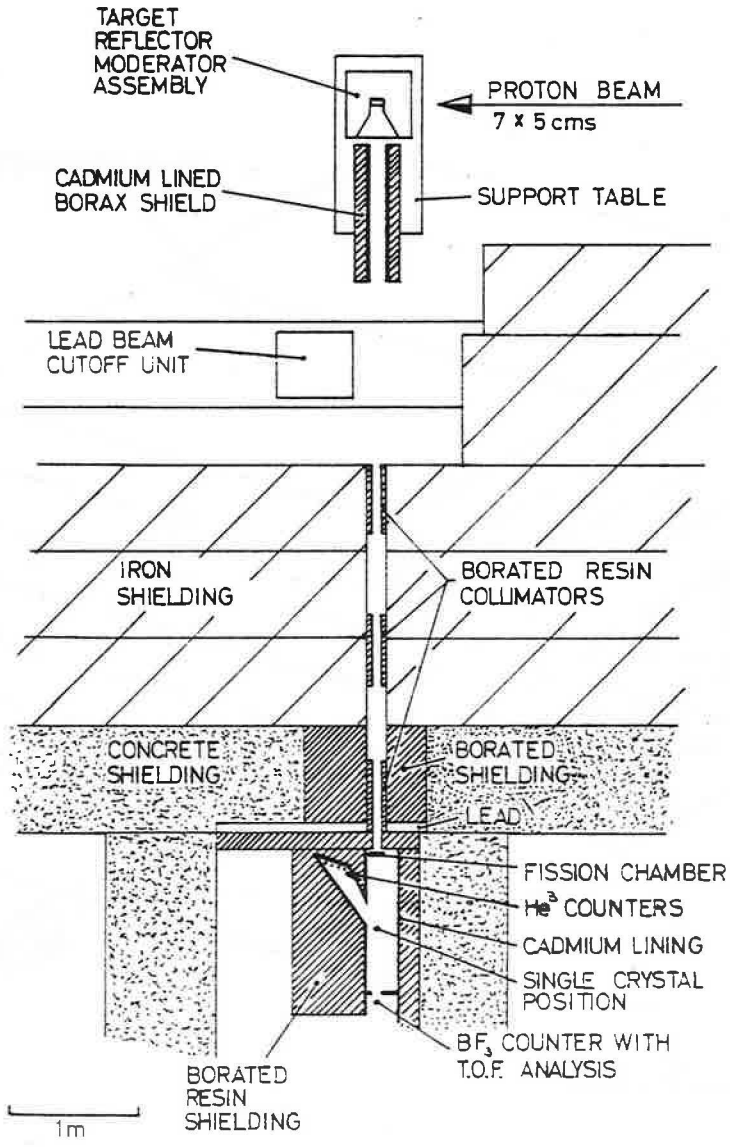

Figure 6. Plan view of the neutron beam area, showing the target-reflector-moderator assembly, collimation arrangement and spectrometer layout.

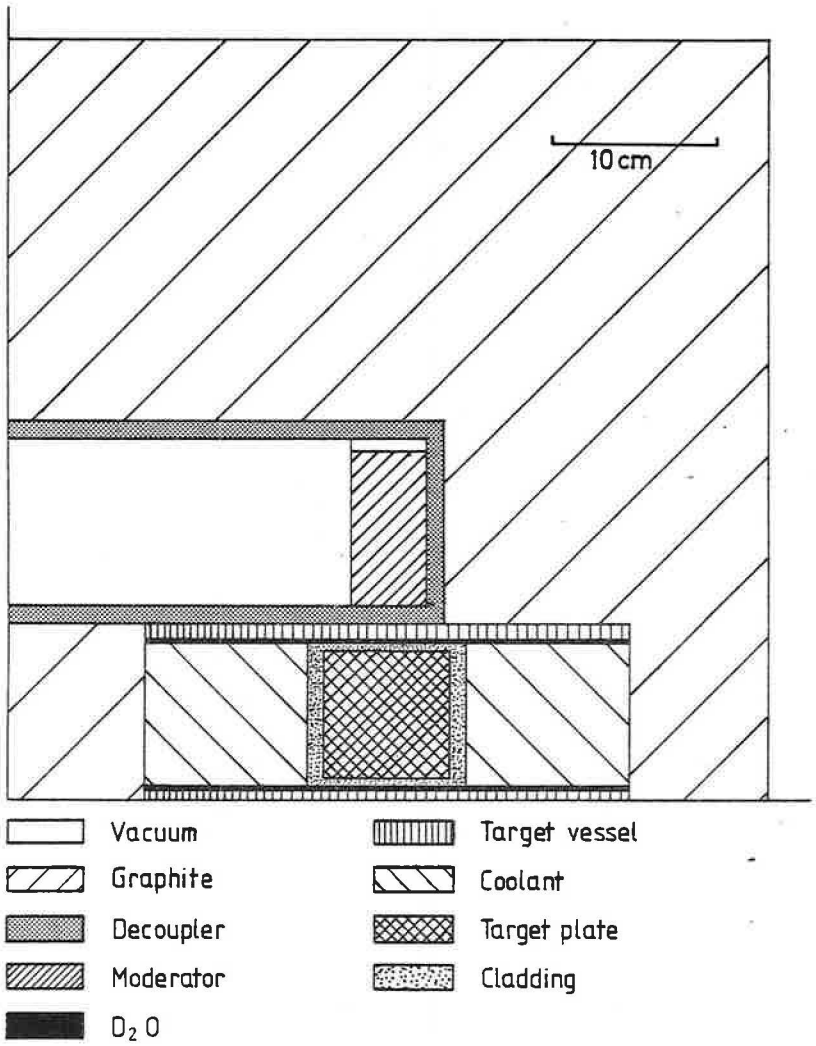

Figure 9. A vertical section through the computer geometry for Large Graphite Reflector. Note that the target and cooling wings take up a large portion of the space available for reflector in the neighbourhood of the moderator.

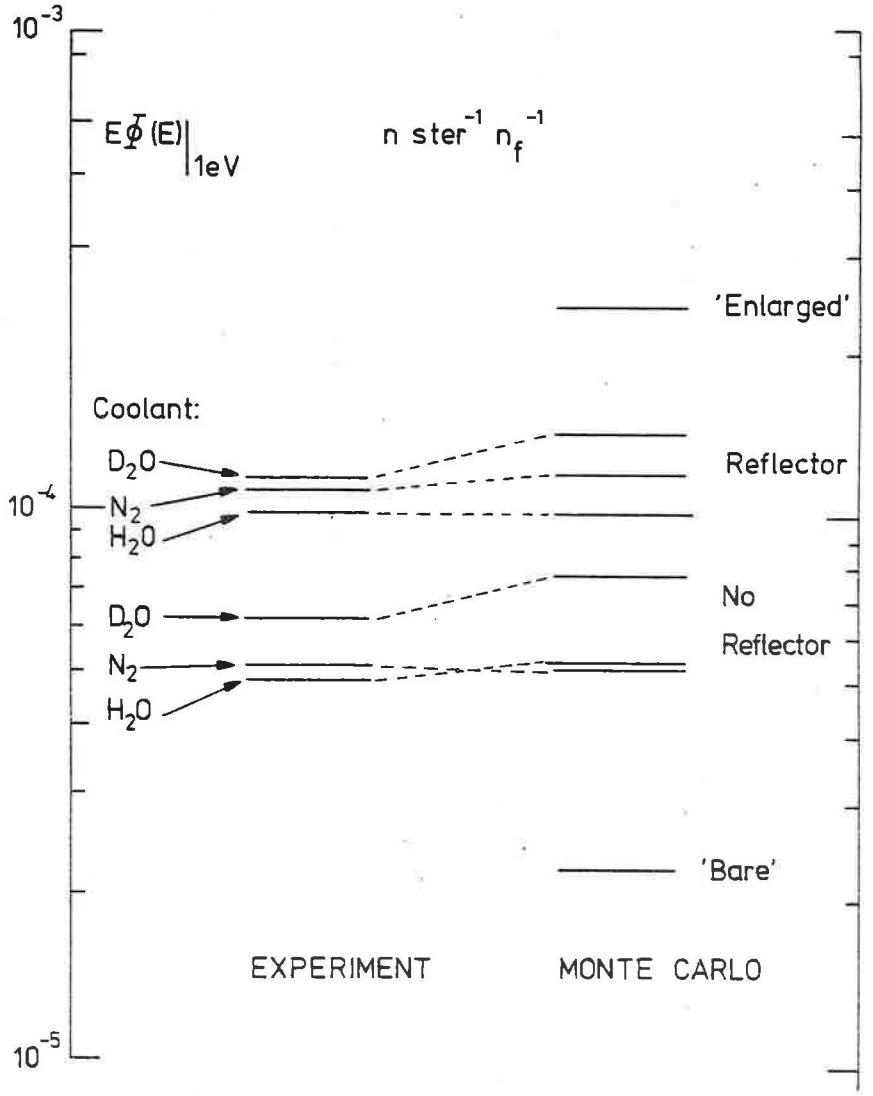

Figure 10. A comparison of the experimental and Monte-Carlo coupling efficiencies for the Large Graphite Assembly with carious coolants. Note that there is a gain of ∿ 10 between the 'Bare' and'Enlarged' simulations.

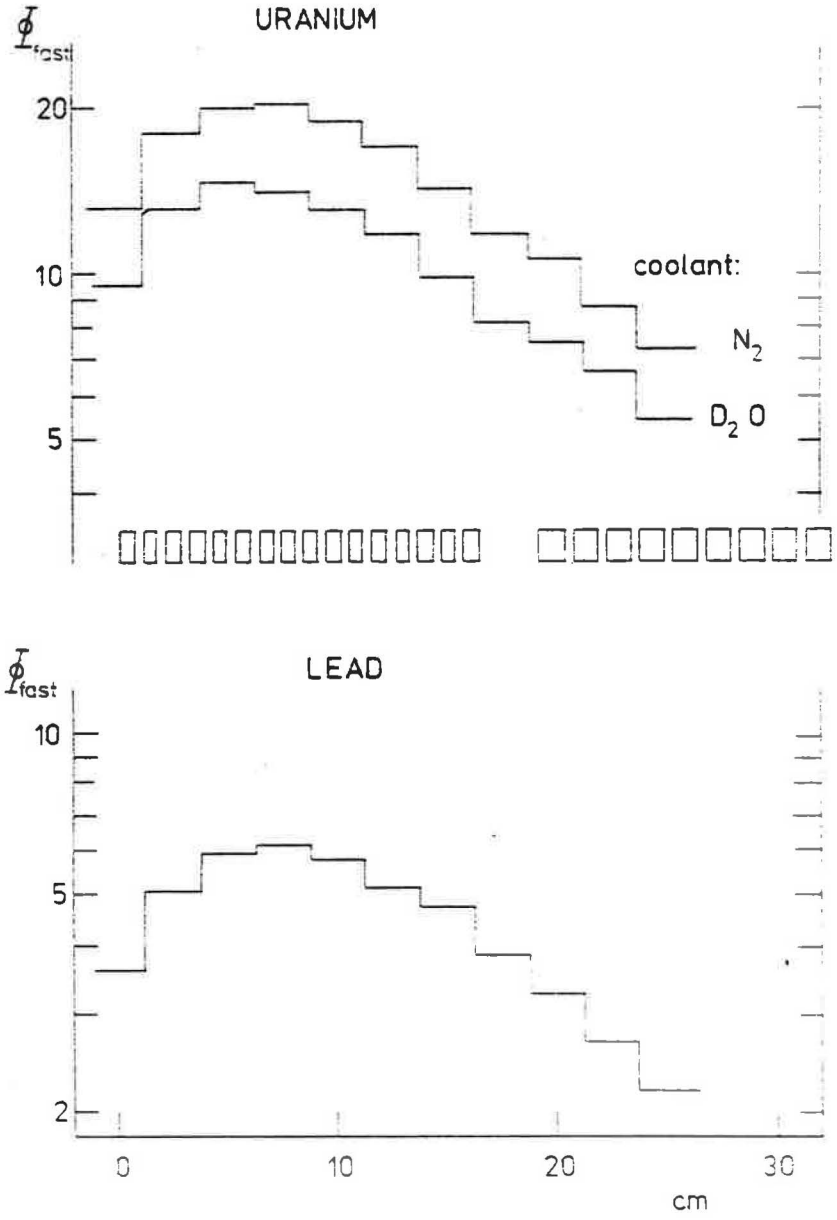

Figure 11. The axial distribution of fast beutrons (as measured by S^{32} activation) for the uranium target (N_2 and D_2O cooled) and a solid lead target. The location of the 16 thin and 9 thick plates of the uranium target is illustrated.

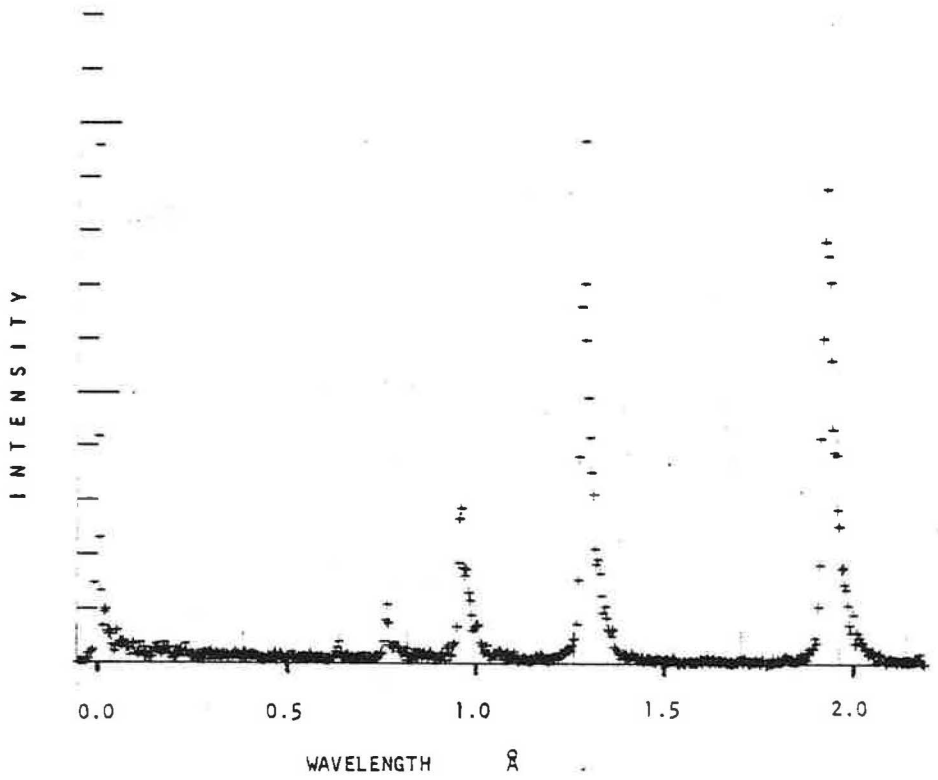

Figure 12. The time-of-flight diffraction pattern from the (220) set of planes of a single crystal of germanium.

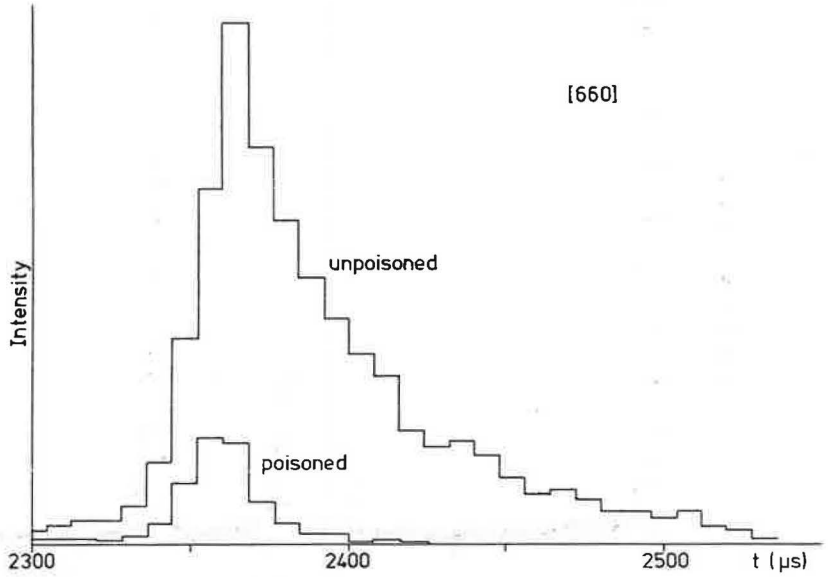

Figure 13. A comparison of the (660) reflection of germanium obtained with a poisoned and an unpoisoned H_2O moderator.